

Electrophysiological properties of human mesenchymal stem cells

Jürgen F. Heubach¹, Eva M. Graf¹, Judith Leutheuser¹, Manja Bock¹, Bartosz Balana¹, Ihor Zahanich¹, Torsten Christ¹, Sabine Boxberger², Erich Wettwer¹ and Ursula Ravens¹

¹Institut für Pharmakologie und Toxikologie, and ²Medizinische Klinik und Poliklinik I, Medizinische Fakultät Carl Gustav Carus der TU Dresden, D-01307 Dresden, Germany

Human mesenchymal stem cells (hMSC) have gained considerable interest due to their potential use for cell replacement therapy and tissue engineering. One strategy is to differentiate these bone marrow stem cells *in vitro* into cardiomyocytes prior to implantation. In this context ion channels can be important functional markers of cardiac differentiation. At present there is little information about the electrophysiological behaviour of the undifferentiated hMSC. We therefore investigated mRNA expression of 26 ion channel subunits using semiquantitative RT-PCR and recorded transmembrane ion currents with the whole-cell voltage clamp technique. Bone marrow hMSC were obtained from healthy donors. The cells revealed a distinct pattern of ion channel mRNA with high expression levels for some channel subunits (e.g. Kv4.2, Kv4.3, MaxiK, HCN2, and $\alpha 1C$ of the L-type calcium channel). Outward currents were recorded in almost all cells. The most abundant outward current rapidly activated at potentials positive to +20 mV. This current was identified as a large-conductance voltage- and Ca^{2+} -activated K^+ current, conducted by MaxiK channels, due to its high sensitivity to tetraethylammonium ($IC_{50} = 340 \mu M$) and its inhibition by 100 nM iberiotoxin. A large fraction of cells also demonstrated a more slowly activating current at potentials positive to –30 mV. This current was selectively inhibited by clofilium ($IC_{50} = 0.8 \mu M$). Ba^{2+} inward currents, stimulated by 1 μM BayK 8644 were found in a few cells, indicating the expression of functional L-type Ca^{2+} channels. Other inward currents such as sodium currents or inward rectifier currents were absent. We conclude that undifferentiated hMSC express a distinct pattern of ion channel mRNA and functional ion channels that might contribute to physiological cell function.

(Resubmitted 25 September 2003; accepted after revision 23 October 2003; first published online 24 October 2003)

Corresponding author U. Ravens: Institut für Pharmakologie und Toxikologie, Medizinische Fakultät Carl Gustav Carus der TU Dresden, Fetscherstrasse 74, D-01307 Dresden, Germany. Email: ravens@rcs.urz.tu-dresden.de

The bone marrow stem cell pool is a rich source of undifferentiated cells that may play a role in physiological tissue restoration (Caplan, 1991; Orlic *et al.* 2002). Two subpopulations of stem cells can be distinguished, the haematopoietic and stromal (mesenchymal) stem cells. The adult bone marrow stem cells have gained much interest as starting material for tissue engineering and cell therapy. Aspiration and defined processing of human bone marrow allows the expansion of a multipotent cell population, the human mesenchymal stem cells (hMSC; Pittenger *et al.* 1999). The cells can be used for *in vitro* studies, where differentiation into osteogenic (Haynesworth *et al.* 1992), chondrogenic (Mackay *et al.* 1998; Winter *et al.* 2003) and adipogenic (Janderova *et al.* 2003) lineage can be readily achieved.

There is evidence that hMSC can also obtain the characteristics of excitable cells. hMSC have the capability of differentiating into cells with a neurone-like phenotype both *in vitro* (Kim *et al.* 2002) and *in vivo* (Zhao *et al.* 2002), and implantation into the ischaemic brain of rats improved functional performance of the apoplectic animals (Zhao *et al.* 2002). In addition, hMSC might be a suitable cell source for cardiac tissue repair in patients with myocardial infarction or heart failure. It has been shown that hMSC injected into the ventricles of immunodeficient mice engrafted into the myocardium and appeared to differentiate into cardiomyocytes, albeit with low frequency (Toma *et al.* 2002). In a swine myocardial infarction model injection of hMSC into the region of myocardial infarction reduced the extent of wall thinning and improved contractile dysfunction (Shake

et al. 2002). Based on these findings it was proposed that hMSC would be useful for cardiomyoplasty (Cahill *et al.* 2003).

Meanwhile, cell therapy for the treatment of ischaemic heart disease has advanced to early clinical studies. In patients with myocardial infarction, bone marrow cells were obtained and injected into the infarct-related coronary artery using a balloon catheter (Assmus *et al.* 2002; Strauer *et al.* 2002). Other groups implanted the cells into ischaemic myocardium by means of a catheter-directed intramural injection (Tse *et al.* 2003) or directly injected cells into the infarct border zone during open heart surgery (Stamm *et al.* 2003). All four studies report an improvement of myocardial perfusion or functional parameters. With the exception of one study (Stamm *et al.* 2003), the mononuclear bone marrow cell suspension employed for cardiac injection was highly heterogeneous, and the used cell populations varied greatly among these clinical studies.

Up to now, enhanced incidence of arrhythmias in patients who received cardiac implantation of bone marrow stem cells has not been noted, although such risk cannot be excluded (Al-Radi *et al.* 2003). Cardiomyocytes derived from human embryonic stem cells have the potential to generate arrhythmic action potentials under some conditions (Zhang *et al.* 2002). At present there is little information about the electrophysiological properties of human bone marrow stem cells. We therefore studied the population of hMSC isolated in our laboratory from bone marrow samples. Commercially available hMSC were used for comparison. We investigated whether undifferentiated hMSC express ion channel mRNA and whether the cells have functional ion currents.

Methods

Isolation of hMSC and cell culture conditions

All parts of this study, especially isolation of human mesenchymal stem cells (hMS) were performed according to the Declaration of Helsinki. The study was approved by the local ethics committee and written informed consent was obtained from donors of bone marrow and cardiac samples. Bone marrow samples were collected from 16 healthy donors at the Mildred Scheel Bone Marrow Transplantation Center of the University Clinics, Dresden hMSC were isolated and cultured according to modifications of previously reported methods (Haynesworth *et al.* 1992; Pittenger *et al.* 1999). Briefly, an aliquot from bone marrow aspirate diluted with PBS–0.5% human serum albumin (HSA) was layered over a Percoll solution ($d = 1.073 \text{ g ml}^{-1}$,

Biochrom, Germany) and centrifuged at 900 g for 30 min. Mononuclear cells at the interface were recovered, washed twice in PBS–HSA and seeded into 75 cm^2 flasks containing Dulbecco's modified Eagle's medium (DMEM, low glucose) supplemented with 2 mM GlutaMAX, 10 U ml^{-1} penicillin, $100 \mu\text{g ml}^{-1}$ streptomycin (all from Gibco Invitrogen, UK) and 10% fetal calf serum (Biochrom). The medium was completely changed after 24 h. After automatic counting cells were maintained in a humidified atmosphere at 5% CO_2 and 37°C until reaching 90% confluency. For subcultivation the cells were replated at a density of $5000 \text{ cells cm}^{-2}$ (Bruder *et al.* 1997). Aliquots of different passages were used for flow-cytometric characterization of the cells (FACS caliber 3CS, Becton Dickinson).

In addition to hMSC isolated in our laboratory we investigated commercially available hMSC (Poietics, BioWhittaker, San Diego, CA, USA) for comparison. These hMSC originated from three Caucasian female donors aged 18, 19 and 26 years (lot numbers 0F2014, 1F0658 and 1F1061). The cells were obtained from the supplier in the 1st or 2nd passage and were certified by the following surface markers: $\text{CD}29^+$, $\text{CD}44^+$, $\text{CD}105^+$, $\text{CD}166^+$ (each $> 95\%$) and $\text{CD}14^-$, $\text{CD}34^-$, $\text{CD}45^-$ (each $< 1\%$). hMSC from BioWhittaker were cultured with the respective mesenchymal stem cell growth medium (hMSCGM; BioWhittaker). mRNA was extracted from subconfluent 4th passages and patch clamp experiments were performed on cells from the 3rd to 6th passage.

Electrophysiological recordings

Membrane currents were measured in the whole cell configuration of the patch clamp technique at $21\text{--}23^\circ\text{C}$ (Hamill *et al.* 1981). Initially, we tried to record currents of hMSC attached to glass cover slips. However, electrophysiological analysis was not feasible under these conditions. We therefore detached subconfluent hMSC from small culture flasks (T25, Greiner, Frickenhausen, Germany) using trypsin–EDTA. After centrifugation at 88 g for 5 min cells were recovered in culture medium. The suspension was stored at room temperature and used within 6 h.

For electrophysiological recordings the cells were transferred to a small chamber (Warner Instruments, Hamden, CT, USA) and allowed to attach to the glass bottom for 15 min. Subsequently, the bath was perfused continuously at a rate of 1.8 ml min^{-1} . Ion channel blockers were applied with the use of a magnet valve or with a rapid solution exchanger (DAD-12 superfusion system, ALA Scientific Instruments,

Table 1. Primer pairs and conditions for PCR

Gene	Acc. no.	Forward primer sequence (5'–3')	Reverse primer sequence (5'–3')	Binding position	Length (bp)	Cycle no.	Reference
α 1C	L29534	TGA GAC CGA GTC CGT CAA A	GAA AAT CAC CAG CCA GTA GAA GA	1333–1522	190	30	Grammer <i>et al.</i> 2000
α 1D	M83566	GCA AGA TGA CGA GCC TGA G	ATG GTT ATG ATG GTT ATG ACA C	5164–5407	244	30	
α 1G	AF134986	ATG GCC ATG GAG CAC TAC C	CGA GGC GTT GAC CTC GAT T	4882–5100	219	30	Huang <i>et al.</i> 2000
α 1H	AF051946	CAC TCA TTC TAC AAC TTC ATC	CTC TCC CGC TGC TTC GTC	1250–1368	190	30	
α 1S	L33798	GGT GGA GGC TGC GAT GGA	ATG GCT GTT GCT ATG GTT GCT	4989–5262	274	30	Barry, 2000
GAPDH	J02642	AAC AGC GAC ACC CAC TCC TC	GGA GGG GAG ATT CAG TGT GGT	869–1126	258	29	
HGN1	AF064876	TTG TCG TCT TTA CTC ACT TTC	CTC CTG ATT GTT GAA AAC AC	1311–1491	181	30	
HGN2	AJ012582	GCC TGA TCC GCT ACA TCC A	TGC GAA GGA GTA CAG TTC AC	1078–1304	227	30	Ludwig <i>et al.</i> 1999
HGN4	AJ132429	CGC CTC ATT CGA TAT ATT CAC	CGC GTA GGA GTA CTG CTT C	1743–1970	228	30	Ludwig <i>et al.</i> 1999
Kir2.1	L36069	GAC CTG GAG ACG GAC GAC	AGC CTG GAG TCT GTC AAA GTC	910–1302	393	30	Wang <i>et al.</i> 1998b
Kir2.2	U16861	TTG AGT AAA CAG GAC ATT GAC	CTG GTT GTG AAG GTC TAT G	1171–1560	390	30	Wang <i>et al.</i> 1998b
Kir2.3	S72503	TAT GGC ATG GGC AAG GAG	AGC TGC CTC CTC CTC CAT C	912–1274	363	30	Wang <i>et al.</i> 1998b
Kir3.1	U50964	TCC CCT TGA CCA ACT TGA ACT	ACG ACA TGA GAA GCA TTT CCT C	928–1301	374	30	Wang <i>et al.</i> 1998b
Kir3.4	U52154	TTT TCC AAC AAC GCA GTC A	CAC AAC TTC AAA CTC TTC C	983–1285	303	30	
Kv1.1	L02750	CCA TCA TTC CTT ATT TCA TCA C	CTC TTC CCC CTC AGT TTC TC	782–1269	488	30	
Kv1.4	L02751	GAG AGA AGA GGA AGA CAG GGC	TGG GGT GCT GAA GTA TCA TTC	828–1073	246	34	Ohya <i>et al.</i> 1997
Kv1.5	M83254	CAT TGC CCT GCC TGT GCC	TGC TCC CGC TGA CCT TCC	1677–1834	158	34	
Kv2.1	L02840	TAC TGG GGC ATC GAC GAG A	GAC TGG CCG AAC TCA TCG A	547–854	308	34	Schultz <i>et al.</i> 2001
Kv3.1	S56770	AGG ACG AGC TGG AGA TGA CC	AAG AAG AGG GAA GCG AAG G	505–664	160	35	Wulfsen <i>et al.</i> 2000
Kv4.2	AJ010969	ATC TTC CGC CAC ATC CTG AA	GAT CCG CAC GGC ACT GTT TC	700–1061	362	34	Postma <i>et al.</i> 2000
Kv4.3	AF205857	GAT GAG CAG ATG TTT GAG CAG	AGC AGG TGG TAG TGA GGC C	1534–1639	106	28	
Kv7.1	U89364	CAT CAT CGA CCT CAT CGT GG	TTC TCG GCA GCA TAG CAC CT	399–959	561	30	Lai <i>et al.</i> 1999
Kv7.2	AF033348	GGA CTC GCT TTC AGG AAG G	CCC TTC CCC TTG GCA G	1331–1494	164	35	
Kv7.3	AF033347	GGA GAG GAG ATG AAA GAG GAG	TGA AGA AAG GAA AAG AGA CGA C	736–1093	358	35	
MaxiK	U11058	ACA ACA TCT CCC CCA ACC	TCA TCA CCT TCT TTC CAA TTC	1222–1531	310	35	
SCN5A	M77235	CCT AAT CAT CTT CCG CAT CC	TGT TCA TCT CTC TGT CCT CAT C	2814–3022	208	35	
Twik1	U336321	TCC TGC TTC TTC TTC ATC	AGG CTC ATT TTG CTT CTG GTC	759–1143	385	30	Wang <i>et al.</i> 1998b

The table specifies forward and reverse primers used for semi-quantitative RT-PCR of various ion channels and the primers for the housekeeping gene glyceraldehyde-3-phosphate dehydrogenase (GAPDH). Primers were constructed with HUSAR program package (Senger *et al.* 1998) or modified using published sequences. Annealing temperature (T_A) was 60°C for all primers except for Kv7.2 (54°C) and Kv7.3 (58°C). After initial denaturation at 94°C for 5 min, cycling conditions were 94°C for 30 s, T_A for 30 s and 72°C for 30 s for all primers except for Kv7.1 (94°C for 60 s, T_A for 60 s and 72°C for 60 s) and Kv7.3 (94°C for 30 s, T_A for 30 s and 72°C for 60 s). Numbers of cycles are indicated for each primer pair. For a final extension reaction mixes were heated at 72°C for 7 min.

Westbury, NY, USA). Membrane currents were measured with a List EPC-7 amplifier (List Medical Instruments, Darmstadt, Germany) under the control of pCLAMP 5.5 software (Axon Instruments, Foster City, CA, USA). Patch electrodes were pulled with a horizontal puller (Zeitz, München, Germany) from filamented borosilicate glass. The tip resistance was 1.5–4.0 M Ω , when filled with electrode solution. Membrane capacitance was measured with fast depolarizing ramp pulses (from –55 to –50 mV, duration 5 ms) at the beginning of each experiment as previously described (Heubach *et al.* 1999). Series resistance was routinely checked and compensated by 50–70%. Membrane currents were low-pass filtered at 2 kHz.

Outward currents were recorded with the following bath solution (mM): NaCl 150, KCl 5.4, CaCl₂ 2, MgCl₂ 2, glucose 11, HEPES 10 (pH 7.4 adjusted with NaOH). The pipette solution included (mM): NaCl 8, KCl 40, potassium aspartate 100, Tris-GTP 0.1, Mg-ATP 5, CaCl₂ 2, EGTA 5 (pH adjusted to 7.3 with KOH) resulting in a calculated free Ca²⁺ and Mg²⁺ concentration of 64 nM and 587 μ M, respectively (Fabiato & Fabiato, 1979). Solutions containing different concentrations of tetraethylammonium chloride were prepared by mixing bath solution as described above with a bath solution in which 20 mM NaCl was replaced by 20 mM tetraethylammonium chloride, in order to keep osmolarity constant. All membrane potentials were corrected for a calculated liquid junction potential of 12.5 mV (JPCalc version 2.2; Barry, 1994). The stimulation frequency was 0.25 Hz. Current amplitude was determined at the end of individual depolarizing steps.

The presence of functional Ca²⁺ channels was assessed with Na⁺-free external solution supplemented with 2 mM Ca²⁺ or 10 mM Ba²⁺ under conditions previously described (Heubach *et al.* 2000). Inward rectifier currents were measured in 20 mM K⁺ solution with ramp pulses from –100 mV to +40 mV of 1250 ms duration from a holding potential of –80 mV as used for the recording of inward rectifier currents in human atrial myocytes (Dobrev *et al.* 2000). In order to enhance the ATP-sensitive potassium current ($I_{K,ATP}$), if present, the intrapipette Mg-ATP concentration was reduced to 0.1 μ M. The presence of hyperpolarization-activated currents was investigated as described for mouse ventricular myocytes (Graf *et al.* 2001). Membrane potential was hyperpolarized for 2 s by steps to –140 mV from a holding potential of –40 mV.

Isolation of RNA and polymerase chain reaction experiments

Total RNA (0.5 μ g) isolated by the guanidinium method (Chomczynski & Sacchi, 1987) was reverse transcribed in a

21 μ l reaction mixture that contained 75 mM KCl, 50 mM Tris-HCl (pH 8.3), 3 mM MgCl₂, 0.5 mM of each dATP, dCTP, dGTP, dTTP, 600 ng of random hexamer primers, 10 mM DTT, 2 U of RNase inhibitor and 10 U of Superscript RNase H⁻ (Invitrogen, Karlsruhe, Germany) according to the manufacturer's instructions. For PCR experiments 3 μ l aliquots of total cDNA were amplified (Master Cycler, Eppendorf, Hamburg, Germany) in a 25 μ l reaction mixture containing 50 mM KCl, 10 mM Tris-HCl (pH 8.3), 1.5 mM MgCl₂, 0.2 mM of each dATP, dCTP, dGTP, dTTP, 25 pmol of each forward and reverse primer and 1.25 U of *Taq* polymerase (Applied Biosystems, Weiterstadt, Germany; for primers and reaction conditions see

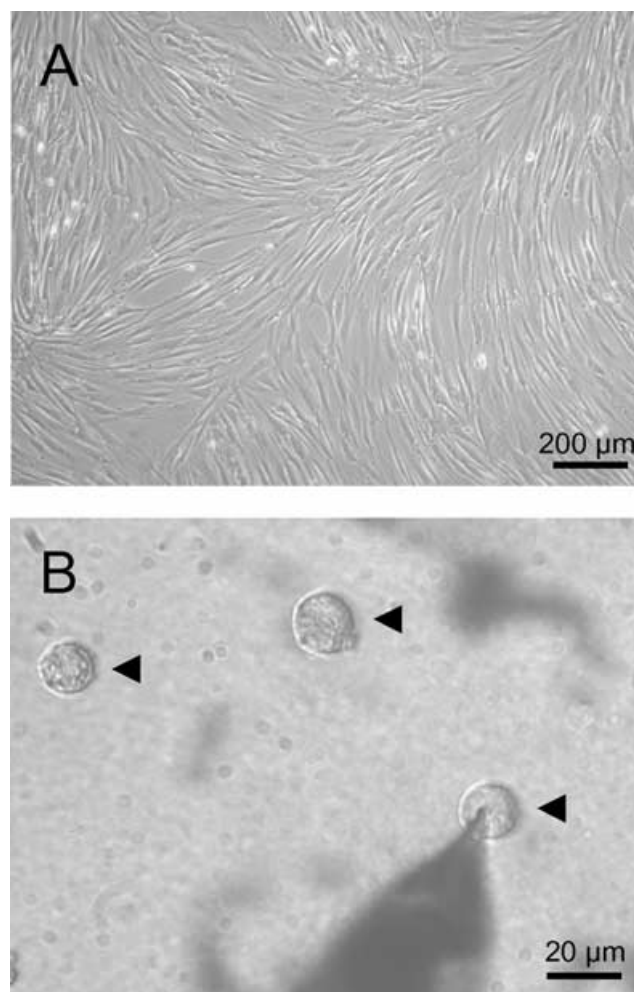


Figure 1. Morphology of human mesenchymal stem cells (hMSC)

A, subconfluent culture with characteristic morphology of adherent cells. *B*, ball-shaped cells after detachment from culture-flasks by trypsin-EDTA treatment and 15 min attachment to the glass bottom of the patch-clamp chamber. Three hMSC are indicated by arrowheads. The right cell was used for electrophysiological recordings (note the patch-electrode).

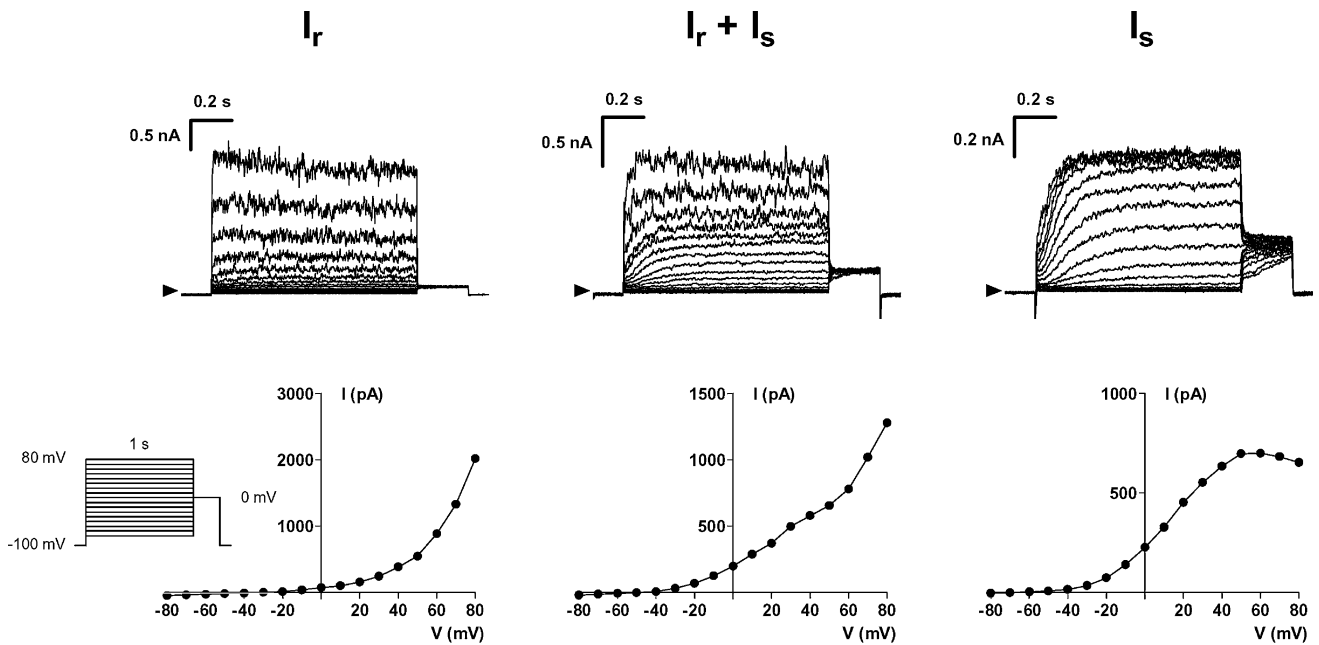


Figure 2. Different patterns of outward currents in hMSC

The top row demonstrates examples of original current traces recorded in three different hMSC, respective current–voltage relations are depicted below. Most of the cells demonstrated a rapidly activating current I_r with noisy current traces at potentials positive to +20 mV (left, a hMSC from 6th passage). The occurrence of a pure slowly activating current I_s was a rare event (right, 5th passage). This current activated at potentials positive to –30 mV and demonstrated saturation at strongly depolarized potentials. In many cells the two currents coexisted (middle, 6th passage) and the ratio between I_r and I_s was highly variable.

Table 1). The same single-stranded cDNA product was used to analyse the expression of all genes described. To ensure that amplification was in the exponential range, the progress of PCR was determined by amplifying identical reaction mixtures for ascending numbers of

cycles. After the cited number of PCR cycles amplification rate was sufficient without reaching saturation for any of the amplicons. PCR products were analysed by agarose gel electrophoresis (2% agarose) and ethidium bromide staining. Bands imaged by a CCD camera (Biostep,

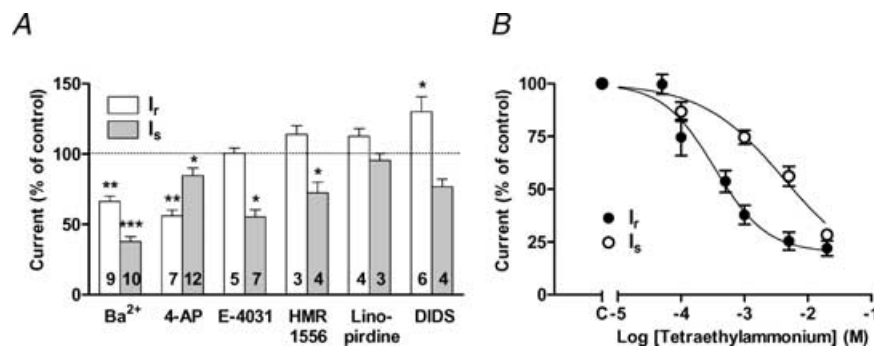


Figure 3. Pharmacological characterization of the two outward currents I_r and I_s

I_r was analysed at the potential +70 mV, whereas I_s was tested at +20 mV to avoid contamination by I_r (see Methods). A, effects of the K^+ channel blockers Ba^{2+} (1 mM), 4-aminopyridine (4-AP, 3 mM), E-4031 (5 μ M), HMR1556 (1 μ M), linopirdine (10 μ M) and of the chloride channel blocker DIDS (200 μ M). Outward current amplitudes in the presence of blockers were normalized to predrug amplitudes. Numbers in columns give the number of cells tested. B, effects of tetraethylammonium on outward current amplitudes. The effects of all compounds were reversible upon washout. * $P < 0.05$, ** $P < 0.01$, *** $P < 0.001$; Student’s paired t test.

Jahnsdorf, Germany) were analysed via optic densitometry with Phoretix 1D software (Biostep).

Chemicals

All chemicals used were of analytical grade and were purchased from commercial suppliers (Sigma, Deisenhofen, Germany, and VWR, Darmstadt, Germany). 4-Aminopyridine, BayK 8644, tetraethylammonium chloride, linopirdine and 4,4'-diisothiocyanatostilbene-

2,2'-disulphonic acid (DIDS) were ordered from Sigma. Clofilium tosylate was from Lilly (Indianapolis, IN, USA), E-4031 was from Eisai Co. (Ibaraki, Japan), and HMR1556 was from Aventis (Frankfurt, Germany). Recombinant iberiotoxin was obtained from Calbiochem (San Diego, CA, USA) and recombinant ergotoxin was ordered from Alomone Laboratories (Jerusalem, Israel). Hanatoxin was a kind gift from Dr Kenton J. Swartz (National Institute of Neurological Disorders and Stroke, NIH Bethesda, MA, USA). Solutions containing peptide

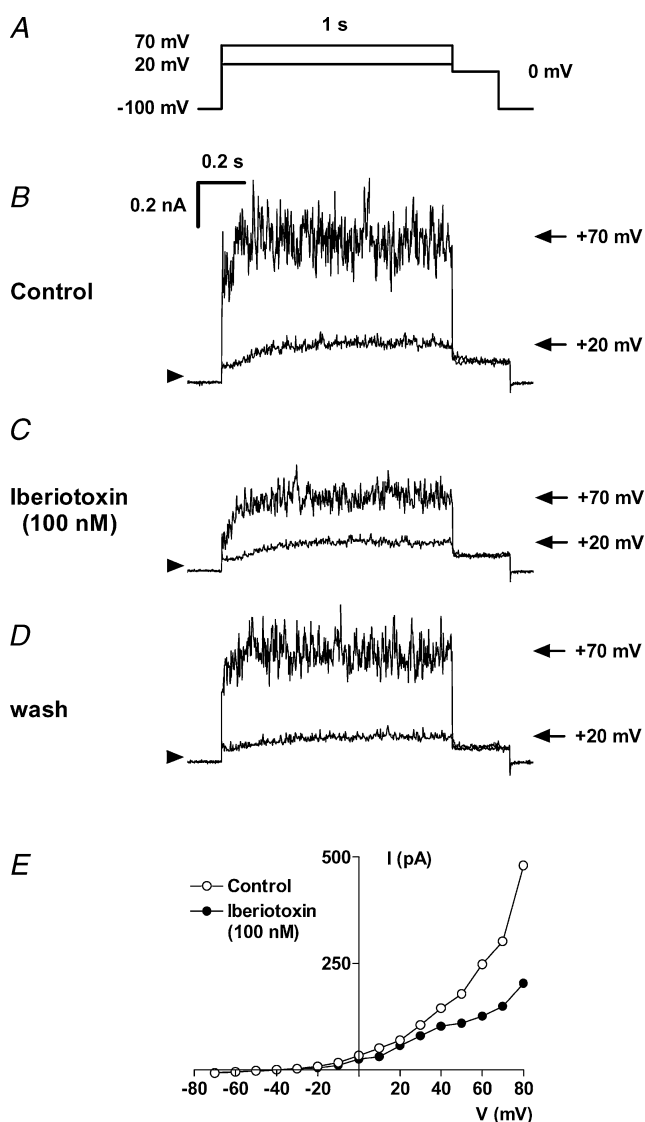


Figure 4. Reversible inhibition of I_r by 100 nm iberiotoxin, a blocker of Ca^{2+} -activated K^+ channels of large conductance A, voltage protocol. Current traces are shown at +20 mV (I_s) and at +70 mV ($I_r + I_s$) under control conditions (B), in the presence of 100 nm iberiotoxin (C) and after washout (D). The current–voltage relation in the absence and presence of iberiotoxin shows selective inhibition of I_r without major block of I_s (E; hMSC from 4th passage).

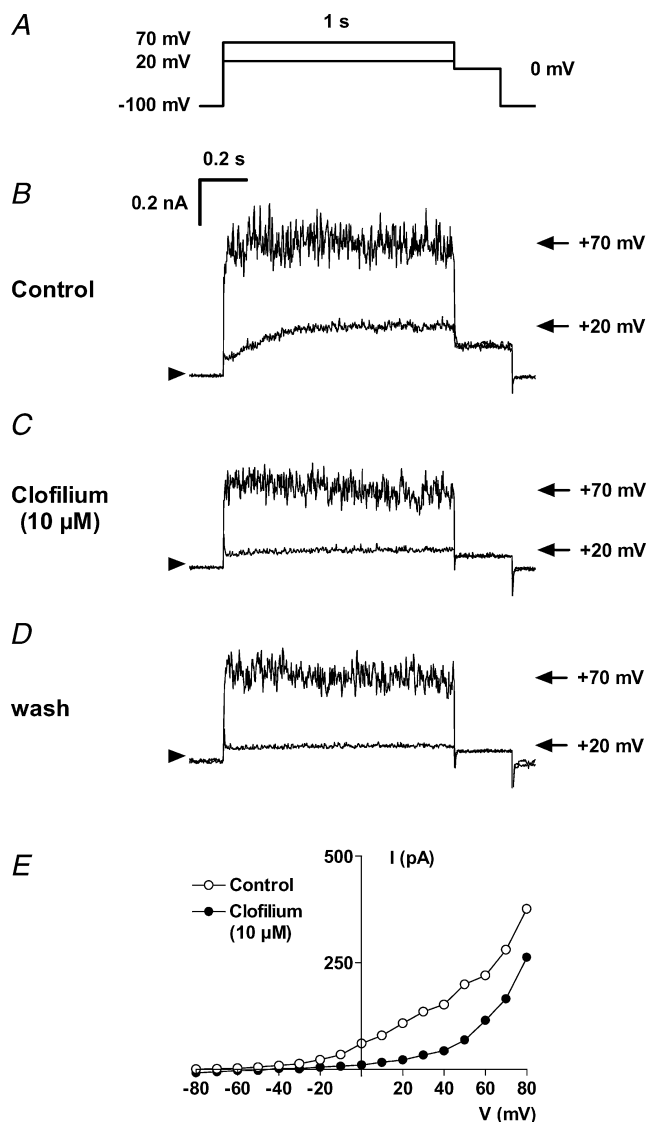


Figure 5. Irreversible block of I_s by 10 μM clofilium, a non-selective blocker of K^+ currents A, voltage protocol. Current traces are shown at +20 mV (I_s) and at +70 mV ($I_r + I_s$) under control conditions (B), in the presence of 10 μM clofilium (C) and after washout (D). The current–voltage relation in the absence and presence of clofilium shows selective inhibition of I_s without major block of I_r (E; hMSC from the 4th passage).

toxins were supplemented with 0.1% bovine serum albumin.

Data analysis and statistics

As shown below we detected two different outward currents (I_r and I_s) in hMSC which variably contributed to total outward current. Differences in voltage dependence of the two currents allowed the classification of hMSC in cells with exclusive occurrence of I_r , I_s or a mixture of both currents. We defined hMSC with exclusive prevalence of I_r current as cells where the ratio between current measured at +20 mV (I_{20}) and current measured at +70 mV (I_{70}) was below 0.25 (compare Fig. 1). A ratio of I_{20} and I_{70} of 0.25–0.5 defined cells with coexistence of both currents and I_{20}/I_{70} above 0.5 defined cells with exclusive occurrence of I_s . Significance of differences between means was tested using Student's paired or unpaired t test with a level of $P < 0.05$ taken to be statistically significant. ANOVA followed by Bonferroni's *post hoc* test was applied in most cases when several groups were compared.

Results

Characterization of hMSC

Human mesenchymal stem cells (hMSC) isolated by our group were characterized by means of flow cytometry. Cells from passages 0 and 1 were positive for CD29 ($93 \pm 2\%$), CD105 ($92 \pm 3\%$), and CD166 ($95 \pm 1\%$), and were negative for CD34 (0%), and CD45 ($2 \pm 1\%$) ($n = 3$ –6 different donors). These levels remained constant during repeated subcultivation up to the last passage (5th)

investigated by flow cytometry. The cultures demonstrated a characteristic growth pattern (Fig. 1A) of a homogeneous cell phenotype. Electrophysiological recordings were performed using ball-shaped cells (Fig. 1B) obtained after trypsin–EDTA treatment of the cultures shown in Fig. 1A.

Outward currents of hMSC

Almost all human mesenchymal stem cells (hMSC) investigated demonstrated outward currents (102 out of 118 cells). Distribution of current patterns and current amplitudes were independent of hMSC source (isolated by our group, $n = 25$ cells *versus* commercial supplier, $n = 77$ cells) and of passage number. Therefore, the pooling of the results for further analysis appeared to be justified.

The most frequently observed current was a rapidly activating outward current which we named I_r (Fig. 2, left). This current activated at potentials positive to +20 mV and only slightly inactivated at positive potentials during prolonged pulses of 1 s duration. Activation of I_r was associated with an increased noise of the current recordings (Fig. 2, left and middle). Tail currents were absent at 0 mV (Fig. 2, left) and also at more negative potentials (data not shown). Mean current density was 16.1 ± 1.8 pA pF⁻¹ at +70 mV in 44 cells that exclusively demonstrated I_r . Forty-nine cells demonstrated an additional current (Fig. 2, middle) that activated at more negative potentials and with slower kinetics. This current is referred to as I_s . Only nine cells exclusively demonstrated this I_s current (Fig. 2, right). I_s did not inactivate and saturated at +50 mV. Mean current density in these nine hMSC was 11.4 ± 1.8 pA pF⁻¹ at +70 mV. Cell capacitance as a measure of cell size was similar in hMSC that

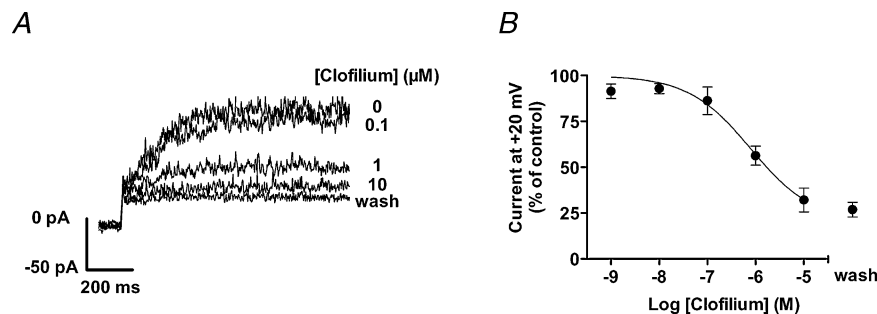


Figure 6. Concentration-dependent block of I_s by clofilium

A, representative current traces at voltage steps from -100 mV to $+20$ mV in the absence and presence of different clofilium concentrations. The inhibition of I_s was not reversible after washout of the drug. B, summary of effects. Inhibition by clofilium was analysed at $+20$ mV to avoid interference from I_r . Up to three increasing concentrations were tested in one cell ($n = 2$ –4 cells per concentration).

exclusively demonstrated I_T (54.1 ± 2.9 pF, $n = 44$) or I_S (54.8 ± 6.7 pF, $n = 9$) or the coexistence of both currents (55.2 ± 3.6 pF, $n = 49$). Membrane potential, however, was significantly more negative in cells

demonstrating I_S current as compared to cells lacking I_S (-35.2 ± 1.6 mV, $n = 29$, versus -28.9 ± 2.1 mV, $n = 17$; $P < 0.05$).

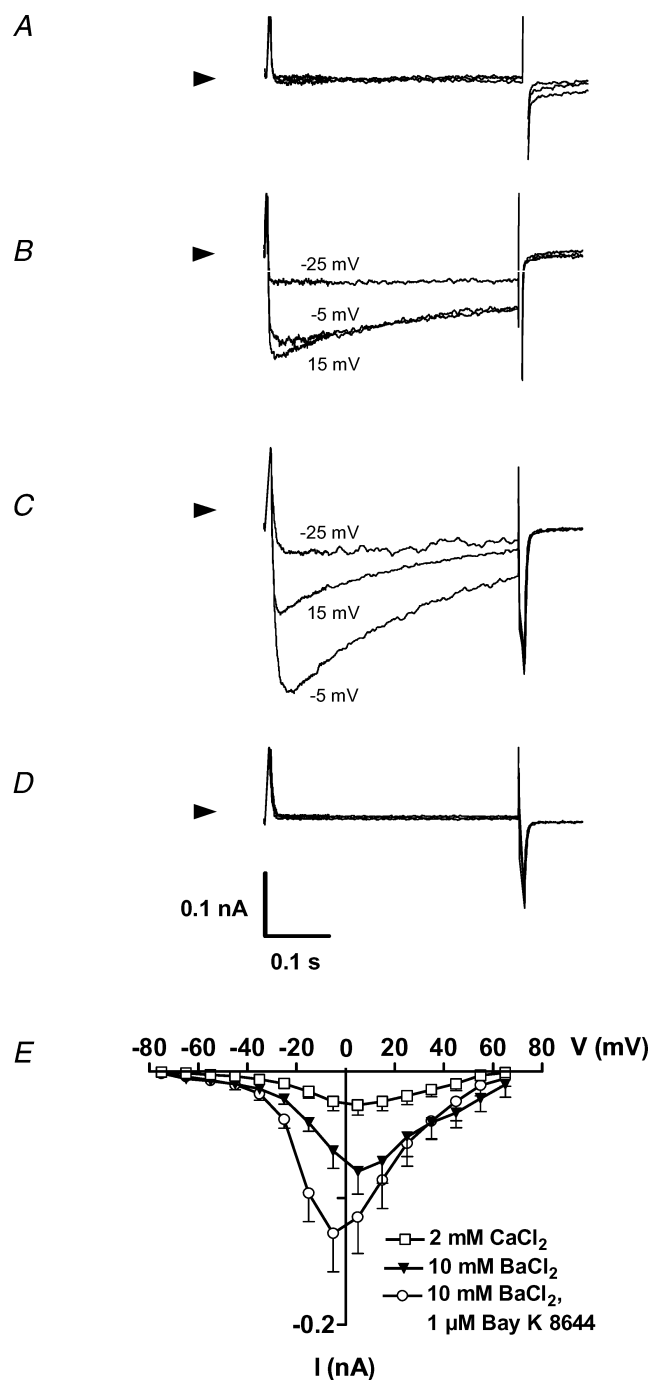


Figure 7. Ca²⁺ and Ba²⁺ currents of hMSC

Original current traces of a representative cell are shown at -25 mV, -5 mV and 15 mV in the presence of 2 mM Ca²⁺ (A), 10 mM Ba²⁺ (B), 10 mM Ba²⁺ plus 1 μM BayK 8644 (C) and 100 μM Cd²⁺ (D). Currents were elicited during 400 ms step depolarizations from a holding potential of -95 mV. Arrowheads indicate zero current.

Current-voltage relations of the Cd²⁺-sensitive currents are shown in (E) for $n = 10$ cells.

Characterization of I_T and I_S

Characterization of the two currents depended on their appropriate separation. Investigation of I_T with pharmacological tools was performed on cells that exclusively demonstrated I_T and currents were analysed at a potential of $+70$ mV (compare Fig. 2, left). However, at $+70$ mV I_S was contaminated by I_T in most cells (Fig. 2, middle). We therefore analysed I_S at $+20$ mV, a potential where I_S amplitude was indeed not at maximum, but free of I_T .

Ba²⁺ significantly blocked both currents, with 1 mM Ba²⁺ having a larger effect on I_S than on I_T (Fig. 3A). 4-Aminopyridine, an unselective blocker of K⁺ currents (3 mM), reduced I_T to approximately 50% but only slightly inhibited I_S . The selective blocker of cardiac delayed rectifier I_{Kr} , E-4031 (5 μM; Sanguinetti & Jurkiewicz, 1990) had no effect on I_T , whereas I_S was reduced by 50%. The highly selective HERG channel blocker ergotoxin (100 nM; Gurrola *et al.* 1999) did not inhibit I_S in three hMSC investigated ($101 \pm 4\%$ of control; data not shown).

A possible relationship of I_S to cardiac delayed rectifier I_{Ks} was tested with HMR1556 (1 μM; Gögelein *et al.* 2000). There was only a slight block of I_S without modulation of I_T (Fig. 3A). Linopirdine (10 μM), which blocks K⁺ channels Kv7.2 and Kv7.3 (i.e. KCNQ2 and 3; Wang *et al.* 1998a), had no effect on I_T and I_S . Hanatoxin, a spider toxin that blocks Kv2.1 channels (Swartz & MacKinnon, 1995) did not block I_S in two cells investigated (data not shown). In addition we investigated the effects of DIDS, a specific inhibitor of cellular anion permeability including Cl⁻ conductance (200 μM; Hume *et al.* 2000). This compound significantly stimulated I_T , but had no effect on I_S (Fig. 3A).

Application of tetraethylammonium chloride markedly reduced the amplitudes of both currents (Fig. 3B). I_S was blocked by tetraethylammonium with half-maximum inhibition at a concentration of 4.1 mM. I_T was found to be more sensitive to this blocker ($IC_{50} = 0.34$ mM), and this, together with other characteristics, suggested that I_T was conducted by voltage- and Ca²⁺-activated K⁺ channels of large conductance (MaxiK).

To identify the channel molecule responsible for I_T we applied iberiotoxin, a selective blocker of MaxiK channels (Galvez *et al.* 1990; Fig. 4). Iberiotoxin (100 nM) inhibited current measured at $+70$ mV to $51 \pm 1\%$ of control amplitude in four cells and the extent of noise, typical for

I_T , was clearly reduced. I_s measured at +20 mV was largely unaffected by iberiotoxin. However, I_s current at +20 mV was irreversibly blocked by clofilium (Castle, 1991) with little effect on I_T (Fig. 5). The IC_{50} value for the inhibition of I_s by clofilium was $0.79 \mu\text{M}$, as shown in Fig. 6.

Inward currents of hMSC

The conditions applied for recording outward currents were also suitable for detecting sodium inward currents, but sodium currents were absent in all cells investigated. In addition we tested for the presence of functional Ca^{2+} channels. At 2 mM external Ca^{2+} it was hard to identify clearly any inward current (Fig. 7A). However, after switching to 10 mM Ba^{2+} , 10 out of 70 cells demonstrated inward currents that were stimulated by $1 \mu\text{M}$ BayK 8644 and completely blocked by $100 \mu\text{M}$ Cd^{2+} (Fig. 7B–D). The currents activated around -35 mV and peaked at -5 to 5 mV (Fig. 7E), consistent with Ba^{2+} currents conducted by L-type Ca^{2+} channels of other cell types. The capacitance of cells with Ba^{2+} currents (116 ± 17 pF) was significantly larger than the capacitance of cells where Ba^{2+} currents were below the limit of detection or absent (67.6 ± 3.8 pF; $P < 0.05$).

Inward rectifier currents were assessed with high external K^+ solution (20 mM, see Methods) to increase K^+ reversal potential and thereby to emphasize the inward

branch of these currents (Dobrev *et al.* 2000). Inward currents were small in amplitude and could hardly be distinguished from putative small leak currents ($n = 11$ cells, data not shown). There were no effects of 1 mM Ba^{2+} , a non-selective blocker of inward rectifier currents. Carbachol ($2 \mu\text{M}$) did not stimulate inward currents, indicating a lack of muscarinic receptors and/or a lack of the acetylcholine-stimulated inward rectifier current $I_{K, \text{ACh}}$. Furthermore, the $I_{K, \text{ATP}}$ channel opener rilmakalim ($10 \mu\text{M}$) and the $I_{K, \text{ATP}}$ channel blocker glibenclamide ($10 \mu\text{M}$) did not modulate inward currents in these 11 cells. The hyperpolarization-activated inward current I_f was absent in five hMSC investigated (data not shown).

mRNA expression of ion channel subunits in hMSC

Finally, we investigated the expression pattern for ion channel isoform mRNA in undifferentiated hMSC. Samples from human atrium and ventricle were taken as control tissues for comparison. hMSC isolated by our group and hMSC obtained from the commercial source exhibited a consistent pattern of ion channel mRNA. Figure 8 demonstrates mRNA expression for ion channel subunits associated with outward currents. There was clear mRNA amplification for Kv4.2 and Kv4.3, two ion channel subunits responsible for transitory outward currents, but

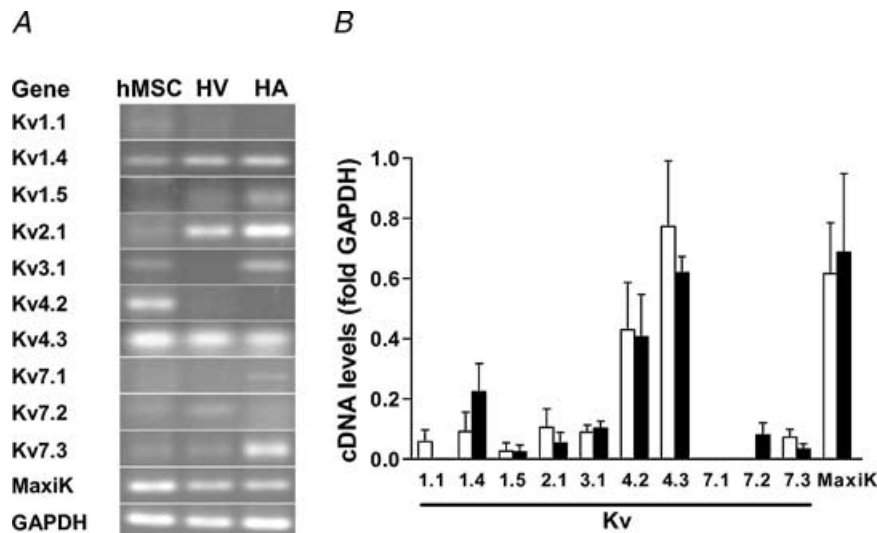


Figure 8. Amplification of mRNA of ion channel subunits related to outward currents by RT-PCR
 A, original gels demonstrating amplification of ion channel subunit transcripts in hMSC, human ventricle (HV) and human atrium (HA). B, summary of amplification with hMSC samples isolated by our group (open bars, $n = 3-5$ donors) and with commercially available hMSC (filled bars, $n = 3$ donors). High mRNA expression levels were detected for channels that conduct transitory outward currents (Kv4.2 and Kv4.3). In addition, MaxiK channels, responsible for large-conductance Ca^{2+} -activated K^+ currents, were strongly expressed. Please note, that despite the absence of, for instance, Kv1.5 in this hMSC sample (A) others did express this channel leading to a small mean value.

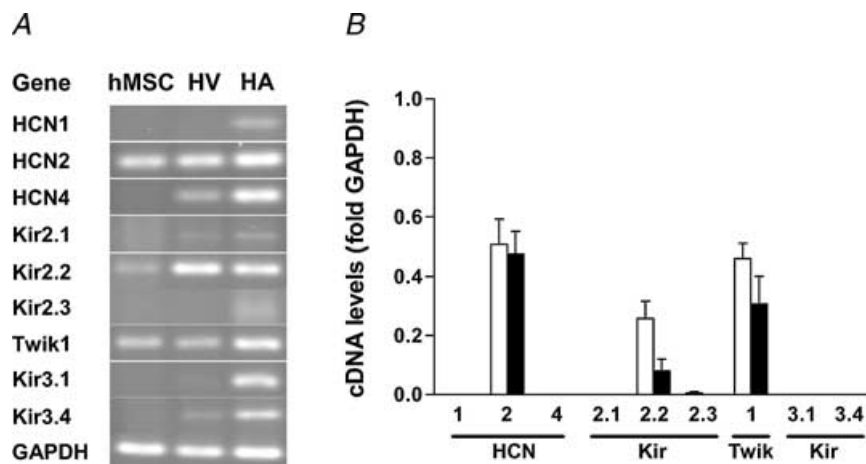


Figure 9. Amplification of mRNA of ion channel subunits related to hyperpolarization-activated inward currents and inward rectifier currents by RT-PCR

A, original gels. *B*, summary of mean values from hMSC samples isolated by our group (open bars, $n = 4$ donors) and from commercially available hMSC (filled bars, $n = 3$ donors). We found strong amplification of cDNA derived from mRNA for the hyperpolarization-activated and cyclic nucleotide-gated channel (HCN) isoform 2 (HCN2), but no amplification for HCN1 and HCN4. High mRNA levels were detected for the two inward rectifier (Kir) subunits Kir2.2 and Twik1, whereas mRNA for the two inward rectifier channels Kir3.1 and Kir3.4 associated with cardiac $I_{K,ACh}$ was absent or below the detection limit.

transient outward currents were not observed in hMSC. However, the high levels of MaxiK mRNA were in line with the detection of an iberiotoxin-sensitive outward current (I_r) in most of the hMSC investigated. In addition we detected low levels of mRNA for Kv1.1, Kv1.4, Kv1.5, Kv2.1, Kv3.1, Kv7.2 and Kv7.3.

mRNA expression levels of channel subunits conducting hyperpolarization-activated currents and inward rectifier currents are shown in Fig. 9. There was strong expression of mRNA for the hyperpolarization-activated and cyclic nucleotide-gated ion channel isoform 2 (HCN2) in all samples of hMSC, but the respective current I_f was not observed (see above). Similarly, there were high levels of mRNA for two channel subunits associated with the inward rectifier current I_{K1} , Kir2.2 and Twik1, but inward rectifier currents were absent. There was

no mRNA expression for Kir3.1 and Kir3.4, responsible for the cardiac acetylcholine-stimulated inward rectifier current $I_{K,ACh}$.

RT-PCR results for Na^+ and Ca^{2+} channel subunits are shown in Fig. 10. mRNA for the Na^+ channel isoform SCN5A was only detected in one sample. However, there was strong expression of the L-type Ca^{2+} channel $\alpha 1C$ subunit in all hMSC samples, whereas mRNA levels for other $\alpha 1$ subunits of the L-type Ca^{2+} channel ($\alpha 1D$, $\alpha 1S$) or T-type Ca^{2+} channel ($\alpha 1G$, $\alpha 1H$) were low or undetectable. As shown in the original gels of Figs 8–10, expression levels for several ion channels were in the same order of magnitude as in tissue samples from human heart. The expression patterns were similar in hMSC isolated by our group and in hMSC obtained from the commercial source.

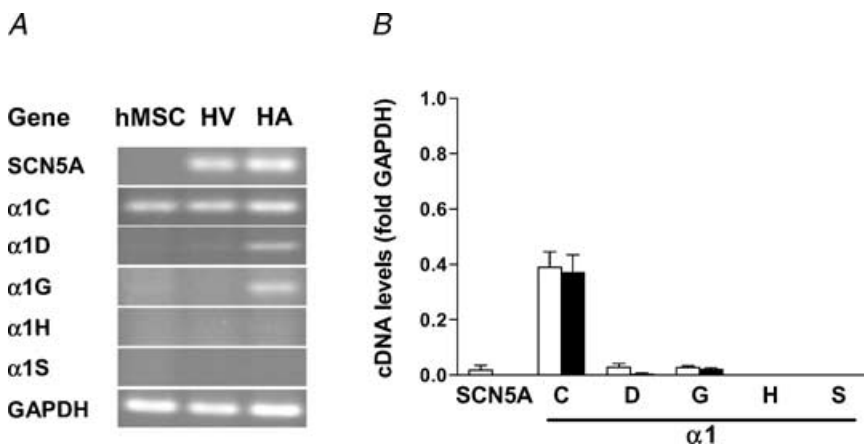


Figure 10. Amplification of mRNA of ion channel subunits related to Na^+ or Ca^{2+} inward currents by RT-PCR

A, original gels. *B*, summary of mean values from hMSC samples isolated by our group (open bars, $n = 4$ –5 donors) and from commercially available hMSC (filled bars, $n = 3$ donors). High expression levels were only found for the $\alpha 1C$ subunit of L-type Ca^{2+} channels.

Discussion

In the context of *in vivo* and *in vitro* differentiation of human mesenchymal stem cells (hMSC) into excitable cells we describe the electrophysiological properties of undifferentiated hMSC. We recorded two distinct outward currents, present either alone or in combination, in almost all cells investigated. A small fraction of cells demonstrated functional Ca^{2+} channels. Semi-quantitative RT-PCR from mRNA of cultured hMSC revealed a consistent expression pattern of ion channel subunits.

Identification of outward currents

Most hMSC demonstrated outward currents that were inhibited by K^+ channel blockers such as Ba^{2+} and 4-aminopyridine, but were not blocked by DIDS, a blocker of Cl^- currents. This general finding suggests that both currents I_r and I_s are carried by K^+ .

The most prevalent outward current of hMSC was I_r , a rapidly activating current which hardly demonstrated any inactivation. One clue towards the identification of its molecular nature is provided by the high sensitivity to tetraethylammonium. There are only a few K^+ channels that are blocked with IC_{50} values around 0.3 mM, namely the Kv1.1 channel, channels of the Kv3 family, Kv7.2 channels and the voltage- and Ca^{2+} -activated K^+ channels of large conductance MaxiK (Rudy & McBain, 2001).

The electrophysiological properties and the pharmacological profiles of Kv1.1, Kv3, and Kv7.2 channels are incongruous with those of I_r current (Coetzee *et al.* 1999). We positively identified I_r as the large-conductance Ca^{2+} -activated K^+ current due to the following additional findings: (i) typical electrophysiological properties, (ii) noisy current traces, which we interpret to be due to large-conductance single channel openings, (iii) sensitivity to iberiotoxin, a specific blocker of MaxiK channels, and finally (iv) high expression levels of MaxiK mRNA in hMSC. MaxiK channels are expressed in many cells and tissues, including neurones, smooth muscle cells and secretory glands (Wallner *et al.* 1999). Moreover, Ca^{2+} -activated K^+ channels were found in osteoblasts (Westkamp *et al.* 2000), adipocytes (Pershadsingh *et al.* 1986), endothelial cells (Wiecha *et al.* 1998) and fibroblasts (Estacion, 1991), i.e. cell types that can be derived from undifferentiated hMSC.

Identification of I_s based on a comparison of its electrophysiological and pharmacological properties with those of known channels is difficult. Slow kinetics of activation suggested some relation to cardiac delayed rectifier I_{Kr} , which is associated with HERG channels, and

I_{Ks} , related to KCNQ1/minK. However, the I_{Kr} blocker E-4031 blocked I_s to a lower extent than expected for the relatively high concentration of 5 μM . In addition, the peptide blocker of I_{Kr} , ergotoxin, had no effect, suggesting that I_s does not flow through HERG channels. The blocker of cardiac I_{Ks} , HMR1556, only affected I_s to a moderate extent. Based on slow activation kinetics and other electrophysiological parameters, Kv2.1, Kv7.2 and Kv7.3 were further candidate molecules for I_s , but hanatoxin and linopirdine did not block this current. It was found that clofilium inhibited I_s with relatively high potency and high selectivity over I_r , and hence can be used in functional experiments for selective suppression of I_s .

Our failure to identify the molecular nature of I_s could be due to the presence of β subunits. The number of possible potassium channel constructs is extended by the presence of β subunits that associate with several pore-forming potassium channel subunits. This association often results in a profound modification of electrophysiological or pharmacological behaviour of the respective current (Nerbonne, 2000). The involvement of one or more β subunits in I_s of hMSC is possible and renders the attribution to known potassium channel subunits even more difficult.

Ion channel mRNA, though expressed at high levels, is not necessarily translated into functionally active channel molecules. The discrepancy between the presence of mRNA but lack of the respective current is most striking for the channel subunits Kv4.2 and Kv4.3, associated with transient outward current I_{to} , but also for the hyperpolarization-activated and cyclic nucleotide-gated channel isoform 2 (HCN2), responsible for the I_f inward current. The reason for the lack of functional channel molecules remains unclear.

Functional role and heterogeneity of ion currents in hMSC

MaxiK channels are sensors of intracellular Ca^{2+} . By this property they regulate membrane potential in a Ca^{2+} -dependent manner (Kawano *et al.* 2003). The activity of MaxiK channels is modulated by phosphorylation via specific receptor-dependent signalling cascades, as recently shown for pathways involving the cellular proto-oncogene pp60 (c-Src; Alioua *et al.* 2002). The large-conductance Ca^{2+} -activated K^+ current could therefore be an effector of trophic factors within the body fluids or cell culture medium.

The functional role of the unidentified I_s current is even more obscure. I_s activates at much more negative

potentials than the large-conductance Ca^{2+} -activated K^{+} current. The presence of I_s should therefore shift the membrane potential of hMSC to more negative potentials. In fact this was observed: hMSC with I_s current had a significantly more negative membrane potential than hMSC without I_s .

Regulation of intracellular calcium in hMSC depends on several mechanisms, and voltage-operated Ca^{2+} currents do not contribute much (Kawano *et al.* 2002; Kawano *et al.* 2003). Only 15% of hMSC demonstrated a small dihydropyridine-sensitive calcium current in the presence of a high external calcium concentration (Kawano *et al.* 2002). This dihydropyridine-sensitive Ca^{2+} current was probably due to the cardiac isoform of the L-type calcium channel, since we found high levels of mRNA for the pore-forming $\alpha 1C$ subunit in hMSC. Our electrophysiological observations confirm the low frequency of hMSC with functional L-type Ca^{2+} channels. Ca^{2+} and Ba^{2+} currents were observed in cells that were significantly larger than cells without these currents. Given a fixed current density, the small current amplitudes would be more easily detectable in large cells. However, this does not completely explain the heterogeneity of Ca^{2+} and Ba^{2+} currents. Heterogeneity was also observed with outward currents, where currents of individual hMSC were not consistent, i.e. some of the cells exclusively showed the large-conductance Ca^{2+} -activated K^{+} current, others expressed I_s current or a mixture of both. Why do individual cells express different currents? There are several possible reasons. Despite the presence of consistent marker proteins on the cell surface and homogeneous morphology of the cultivated cells, the cells investigated possibly did not come from an absolutely homogeneous population of hMSC, but also included fractions of more or less committed progenitor cells (Minguell *et al.* 2001; Muraglia *et al.* 2000). These cell populations could slightly differ in their ion current patterns. Another possible reason is the dependence of ion current expression on cell function. For example, there is evidence that current expression varies at different phases of the cell cycle (Ouadid-Ahidouch *et al.* 2001; Chittajallu *et al.* 2002). Nevertheless, there is only a limited number of different currents observed in undifferentiated hMSC. The modification of present currents and the occurrence of new currents could be suitable markers of *in vitro* hMSC differentiation.

Consequences and perspectives

Preliminary clinical studies have shown that the injection of undifferentiated bone marrow stem cells into the infarcted heart can improve cardiac function. The fate

of the implanted cells, whether they differentiate into cardiomyocytes, contribute to neoangiogenesis, or just perish, remains unclear. The injection transfers the undifferentiated cells, that can well include hMSC, directly into an electrically active environment. We have demonstrated that hMSC express a consistent pattern of ion channels and at least three different ion currents. Therefore, the cells have some bioelectrical activity, as also shown by others (Kawano *et al.* 2002, 2003). Based on our finding we cannot judge whether implantation of hMSC is safe or includes the risk of arrhythmia. However, careful monitoring of the patients will be necessary and will certainly be done, to rule out any pro-arrhythmogenic potential of the undifferentiated hMSC or of the hMSC-derived cardiomyocytes.

References

- Alioua A, Mahajan A, Nishimaru K, Zarei MM, Stefani E & Toro L (2002). Coupling of c-Src to large conductance voltage- and Ca^{2+} activated K^{+} channels as a new mechanism of agonist-induced vasoconstriction. *Proc Natl Acad Sci USA* **99**, 14560–14565.
- Al-Radi OO, Rao V, Li RK, Yau T & Weisel RD (2003). Cardiac cell transplantation: closer to bedside. *Ann Thorac Surg* **75**, S674–S677.
- Assmus B, Schächinger V, Teupe C, Britten M, Lehmann R, Döbert N, Grünwald F, Aicher A, Urbich C, Martin H, Hoelzer D, Dimmeler S & Zeiher A (2002). Transplantation of progenitor cells and regeneration enhancement in acute myocardial infarction (TOPCARE-AMI). *Circulation* **106**, 3009–3017.
- Barry PH (1994). JPCalc, a software package for calculating liquid junction potential corrections in patch-clamp, intracellular, epithelial and bilayer measurements and for correcting junction potential measurements. *J Neurosci Meth* **51**, 107–116.
- Barry EL (2000). Expression of mRNAs for the alpha 1 subunit of voltage-gated calcium channels in human osteoblast-like cell lines and in normal human osteoblasts. *Calcif Tissue Int* **66**, 145–150.
- Bruder SP, Jaiswal N & Haynesworth SE (1997). Growth kinetics, self-renewal and the osteogenic potential of purified human mesenchymal stem cells during extensive subcultivation and following cryopreservation. *J Cell Biochem* **64**, 278–294.
- Cahill KS, Toma C, Pittenger MF, Kessler PD & Byrne BJ (2003). Cell therapy in the heart: cell production, transplantation, and applications. *Meth Mol Biol* **219**, 73–81.
- Caplan AI (1991). Mesenchymal stem cells. *J Orthopaed Res* **9**, 641–650.
- Castle NA (1991). Selective inhibition of potassium currents in rat ventricle by clofilium and its tertiary homolog. *J Pharmacol Exp Ther* **257**, 342–350.

- Chittajallu R, Chen Y, Wang H, Yuan X, Ghiani CA, Heckman T, McBain CJ & Gallo V (2002). Regulation of Kv1 subunit expression in oligodendrocyte progenitor cells and their role in G1/S phase progression of the cell cycle. *Proc Natl Acad Sci USA* **99**, 2350–2355.
- Chomczynski P & Sacchi N (1987). Single-step method of RNA isolation by acid guanidinium thiocyanate-phenol-chloroform extraction. *Anal Biochem* **162**, 156–159.
- Coetzee WA, Amarillo Y, Chiu J, Chow A, Lau D, McCormack T, Moreno H, Nadal MS, Ozaita A, Pountney D, Saganich M, Vega-Saenz de Miera E & Rudy B (1999). Molecular diversity of K⁺ channels. *Ann NY Acad Sci* **868**, 233–285.
- Dobrev D, Wettwer E, Himmel HM, Kortner A, Kuhlisch E, Schuler S, Siffert W & Ravens U (2000). G-protein β 3-subunit 825T allele is associated with enhanced human atrial inward rectifier potassium currents. *Circulation* **102**, 692–697.
- Estacion M (1991). Characterization of ion channels seen in subconfluent human dermal fibroblasts. *J Physiol* **436**, 579–601.
- Fabiato A & Fabiato F (1979). Calculator programs for computing the composition of the solutions containing multiple metals and ligands used for experiments in skinned muscle cells. *J Physiol (Paris)* **75**, 463–505.
- Galvez A, Gimenez-Gallego G, Reuben JP, Roy-Contancin L, Feigenbaum P, Kaczorowski GJ & Garcia ML (1990). Purification and characterization of a unique, potent, peptidyl probe for the high conductance calcium-activated potassium channel from venom of the scorpion *Buthus tamulus*. *J Biol Chem* **265**, 11083–11090.
- Göglein H, Bruggemann A, Gerlach U, Brendel J & Busch AE (2000). Inhibition of I_{Ks} channels by HMR1556. *Naunyn-Schmiedeberg's Arch Pharmacol* **362**, 480–488.
- Graf EM, Heubach JF & Ravens U (2001). The hyperpolarization-activated current I_f in ventricular myocytes of non-transgenic and β ₂-adrenoceptor overexpressing mice. *Naunyn-Schmiedeberg's Arch Pharmacol* **364**, 131–139.
- Grammer JB, Bosch RF, Kühlkamp V & Seipel L (2000). Molecular and electrophysiological evidence for 'remodeling' of the L-type Ca²⁺ channel in persistent atrial fibrillation in humans. *Z Kardiol (Suppl. 4)* **89**, IV/23–IV/29.
- Gurrola GB, Rosati B, Rocchetti M, Pimienta G, Zaza A, Arcangeli A, Olivotto M, Possani LD & Wanke E (1999). A toxin to nervous, cardiac, and endocrine ERG K⁺ channels isolated from *Centruroides noxius* scorpion venom. *FASEB J* **13**, 953–962.
- Hamill OP, Marty A, Neher E, Sakmann B & Sigworth FJ (1981). Improved patch clamp technique for high resolution current recording from cells and cell-free membrane patches. *Pflugers Arch* **391**, 85–100.
- Haynesworth SE, Goshima J, Goldberg VM & Caplan AI (1992). Characterization of cells with osteogenic potential from human marrow. *Bone* **13**, 81–88.
- Heubach JF, Köhler A, Wettwer E & Ravens U (2000). T-type and tetrodotoxin-sensitive Ca²⁺ currents coexist in guinea pig ventricular myocytes and are both blocked by mibefradil. *Circ Res* **86**, 628–635.
- Heubach JF, Trebeß I, Wettwer E, Himmel HM, Michel MC, Kaumann AJ, Koch WJ, Harding SE & Ravens U (1999). L-type calcium current and contractility in ventricular myocytes from mice overexpressing the cardiac β ₂-adrenoceptor. *Cardiovasc Res* **42**, 173–182.
- Huang B, Qin D, Deng L, Boutjdir M & El-Sherif N (2000). Reexpression of L-type Ca²⁺ channel gene and current in post-infarction remodeled left rat ventricle. *Cardiovasc Res* **46**, 442–449.
- Hume JR, Duan D, Collier ML, Yamazaki J & Horowitz B (2000). Anion transport in heart. *Physiol Rev* **80**, 31–81.
- Janderova L, McNeil M, Murrell AN, Mynatt RL & Smith SR (2003). Human mesenchymal stem cells as an in vitro model for human adipogenesis. *Obes Res* **11**, 65–74.
- Kawano S, Otsu K, Shoji S, Yamagata K & Hiraoka M (2003). Ca²⁺ oscillations regulated by Na⁺-Ca²⁺ exchanger and plasma membrane Ca²⁺ pump induce fluctuations of membrane currents and potentials in human mesenchymal stem cells. *Cell Calcium* **34**, 145–156.
- Kawano S, Shoji S, Ichinose S, Yamagata K, Tagami M & Hiraoka M (2002). Characterization of Ca²⁺ signalling pathways in human mesenchymal stem cells. *Cell Calcium* **32**, 165–174.
- Kim BJ, Seo JH, Bubien JK & Oh YS (2002). Differentiation of adult bone marrow stem cells into neuroprogenitor cells in vitro. *Neuroreport* **13**, 1185–1188.
- Lai L-P, Su M-J, Lin J-L, Lin F-Y, Tsai C-H, Chen Y-S, Tseng Y-Z, Lien W-P & Huang SKS (1999). Changes in the mRNA levels of delayed rectifier potassium channels in human atrial fibrillation. *Cardiology* **92**, 248–255.
- Ludwig A, Zong X, Stieber J, Hullin R, Hofmann F & Biel M (1999). Two pacemaker channels from human heart with profoundly different activation kinetics. *EMBO J* **18**, 2323–2329.
- Mackay AM, Beck SC, Murphy JM, Barry FP, Chichester CO & Pittenger MF (1998). Chondrogenic differentiation of cultured human mesenchymal stem cells from marrow. *Tissue Eng* **4**, 415–428.
- Minguell JJ, Erices A & Conget P (2001). Mesenchymal stem cells. *Exp Biol Med* **226**, 507–520.
- Muraglia A, Cancedda R & Quarto R (2000). Clonal mesenchymal progenitors from human bone marrow differentiate in vitro according to a hierarchical model. *J Cell Sci* **113**, 1161–1166.
- Nerbonne JM (2000). Molecular basis of functional voltage-gated K⁺ channel diversity in the mammalian myocardium. *J Physiol* **525**, 285–298.
- Ohya S, Tanaka M, Oku T, Asai Y, Watanabe M, Giles WR & Imaizumi Y (1997). Molecular cloning and tissue distribution of an alternatively spliced variant of an A-type K⁺ channel α -subunit, Kv4.3 in the rat. *FEBS Lett* **420**, 47–53.

- Orlic D, Hill JM & Arai AE (2002). Stem cells for myocardial regeneration. *Circ Res* **91**, 1092–1102.
- Ouadid-Ahidouch H, Le Bourhis X, Roudbaraki M, Toillon RA, Delcourt P & Prevarskaya N (2001). Changes in the K⁺ current-density of MCF-7 cells during progression through the cell cycle: possible involvement of a h-ether.a-gogo K⁺ channel. *Receptor Channel* **7**, 345–356.
- Pershad Singh HA, Gale RD, Delfert DM & McDonald JM (1986). A calmodulin dependent Ca²⁺ activated K⁺ channel in the adipocyte plasma membrane. *Biochem Biophys Res Commun* **135**, 934–941.
- Pittenger MF, Mackay AM & Beck SC (1999). Multilineage potential of adult human mesenchymal stem cells. *Science* **284**, 143–147.
- Postma AV, Bezzina CR, de Vries JF, Wilde AAM, Moorman AFM & Mannens MMAM (2000). Genomic organisation and chromosomal localisation of two members of the KCND ion channel family, KCND2 and KCND3. *Hum Genet* **106**, 614–619.
- Rudy B & McBain CJ (2001). Kv3 channels: voltage-gated K⁺ channels designed for high-frequency repetitive firing. *Trends Neurosci* **24**, 517–526.
- Sanguinetti MC & Jurkiewicz NK (1990). Two components of cardiac delayed rectifier K⁺ current. Differential sensitivity to block by class III antiarrhythmic agents. *J General Physiol* **96**, 195–215.
- Schultz J-H, Volk T & Ehmke H (2001). Heterogeneity of Kv2.1 mRNA expression and delayed rectifier current in single isolated myocytes from rat left ventricle. *Circ Res* **88**, 483–490.
- Senger M, Flores T, Glatting K, Ernst P, Hotz-Wagenblatt A & Suhai S (1998). W2H:WWW interface to the GCG sequence analysis package. *Bioinformatics* **14**, 452–457.
- Shake JG, Gruber PJ, Baumgartner WA, Senechal G, Meyers J, Redmond JM, Pittenger MF & Martin BJ (2002). Mesenchymal stem cell implantation in a swine myocardial infarct model: engraftment and functional effects. *Ann Thorac Surg* **73**, 1919–1925.
- Stamm C, Westphal B, Kleine HD, Petzsch M, Kittner C, Klinge H, Schumichen C, Nienaber CA, Freund M & Steinhoff G (2003). Autologous bone-marrow stem-cell transplantation for myocardial regeneration. *Lancet* **361**, 45–46.
- Strauer BE, Brehm M, Zeus T, Köstering M, Hernandez A, Sorg RV, Kögler G & Wernet P (2002). Repair of infarcted myocardium by autologous intracoronary mononuclear bone marrow cell transplantation in humans. *Circulation* **106**, 1913–1918.
- Swartz KJ & MacKinnon R (1995). An inhibitor of the Kv2.1 potassium channel isolated from the venom of a Chilean tarantula. *Neuron* **15**, 941–949.
- Toma C, Pittenger MF, Cahill KS, Byrne BJ & Kessler PD (2002). Human mesenchymal stem cells differentiate to a cardiomyocyte phenotype in the adult murine heart. *Circulation* **105**, 93–98.
- Tse HF, Kwong YL, Chan JKF, Lo G, Ho CL & Lau CP (2003). Angiogenesis in ischaemic myocardium by intramyocardial autologous bone marrow mononuclear cell implantation. *Lancet* **361**, 47–49.
- Wallner M, Meera P & Toro L (1999). Molecular basis of fast inactivation in voltage and Ca²⁺-activated K⁺ channels: a transmembrane beta-subunit homolog. *Proc Natl Acad Sci USA* **96**, 4137–4142.
- Wang HS, Pan Z, Shi W, Brown BS, Wymore RS, Cohen IS, Dixon JE & McKinnon D (1998a). KCNQ2 and KCNQ3 potassium channel subunits: Molecular correlates of the M-channel. *Science* **282**, 1890–1893.
- Wang Z, Yue L, White M, Pelletier G & Nattel S (1998b). Differential distribution of inward rectifier potassium channel transcripts in human atrium versus ventricle. *Circulation* **98**, 2422–2428.
- Westkamp M, Seidl W & Grissmer S (2000). Characterization of the increase in [Ca²⁺]_i during hypotonic shock and the involvement of Ca²⁺-activated K⁺ channels in the regulatory volume decrease in human osteoblast-like cells. *J Membr Biol* **178**, 11–20.
- Wiecha J, Munz B, Wu Y, Noll T, Tillmanns H & Waldecker B (1998). Blockade of Ca²⁺-activated K⁺ channels inhibits proliferation of human endothelial cells induced by basic fibroblast growth factor. *J Vasc Res* **35**, 363–371.
- Winter A, Breit S, Parsch D, Benz K, Steck E, Hauner H, Weber RM, Ewerbeck V & Richter W (2003). Cartilage-like gene expression in differentiated human stem cell spheroids: a comparison of bone marrow-derived and adipose tissue-derived stromal cells. *Arthritis Rheum* **48**, 418–429.
- Wulfen I, Hauber H-P, Schiemann C, Bauer CK & Schwarz JR (2000). Expression of mRNA for voltage-dependent and inward-rectifying K channels in GH₃/B₆ cells and rat pituitary. *J Neuroendocrinol* **12**, 263–272.
- Zhang YM, Hartzell C, Narlow M & Dudley SC (2002). Stem cell-derived cardiomyocytes demonstrate arrhythmic potential. *Circulation* **106**, 1294–1299.
- Zhao LR, Duan WM, Reyes M, Keene CD, Verfaillie CM & Low WC (2002). Human bone marrow stem cells exhibit neural phenotypes and ameliorate neurological deficits after grafting into the ischemic brain of rats. *Exp Neurol* **174**, 11–20.

Acknowledgements

The excellent technical assistance of Romy Kempe and Silvia Feldmann is gratefully acknowledged. This work was supported by an InnoRegio BioMeT-grant of the Bundesministerium für Bildung und Forschung to B.B., by a grant of the Deutsche Gesellschaft für Kardiologie-Herz-und Kreislaufforschung to I.Z., by a MeDDrive-grant of the Medizinische Fakultät Carl Gustav Carus, Dresden University of Technology, to J.F.H and by a grant of the Sächsische Ministerium für Wissenschaft und Kunst to J.F.H and U.R.